

# 3-Dimensional MULTI-LAYERED 6-VERTEX STATISTICAL MODEL: EXACT SOLUTION

V. Popkov, Center for Theoretical Physics, Seoul National University, Seoul 151-742 Korea  
( on leave from Institute for Low Temperature Physics,  
47 Lenin Ave, 310164 Kharkov, Ukraine)  
B. Nienhuis, Institute for Theoretical Physics (University of Amsterdam)  
Valckernierstraat 65, NL 1018 XE Amsterdam

October 6, 2018

## Abstract

Solvable via Bethe Ansatz (BA) anisotropic statistical model on cubic lattice consisting of locally interacting 6-vertex planes, is studied. Symmetries of BA lead to infinite hierarchy of possible phases, which is further restricted by numerical simulations. The model is solved for arbitrary value of the interlayer coupling constant. Resulting is the phase diagram in general 3-parameter space. Two new phases of chiral (spiral) character and new first order phase transition appear due to the interplane interaction. Exact mapping onto the models with some inhomogeneous sets of interlayer coupling constants is established.

## 1 Introduction

Exactly solvable models e.g. models for which set of physical quantities such as the bulk free energy, the interfacial tension, some critical exponents etc. can be calculated analytically, play important role in statistical mechanics and the phase transitions theory. Most solvable statistical models are two-dimensional (see [1] for review). YBE, or star-triangle equation, serves as integrability condition, or transfer-matrices commutativity condition for  $2D$  solvable models. Unlike  $2D$  models, solvable models in  $3D$  are very rare examples. Usually solvable  $3D$  models — see e.g. Zamolodchikov model [3] and its generalizations [4] — are based on solution of tetrahedron equation. The latter is natural generalization of Yang-Baxter equation YBE and serves as transfer-matrices in  $3D$  commutativity condition.

Unfortunately all  $3D$  solvable models known so far possess common rather unsatisfactory feature, from the viewpoint of applications to statistical mechanics — they incurably have negative [3] or even complex [4] Boltzmann weights. Since these weights are probabilities (up to a normalization), this property makes statistical mechanical interpretation of the models highly problematical (although the associated quantum problem may still be sensible).

Recently the method was proposed in [6, 7] which allows to construct solvable statistical models (however anisotropic) with positive Boltzmann weights and local interactions in  $3D$  starting from solvable  $2D$  models. The idea is the following: the whole row of infinite number of separate sites (vertexes) is considered as a simplest object. The states probabilities (Boltzmann weights) are defined as product of those for each site separately, multiplied by interaction factors depending upon the local configurations of each two neighbouring sites. Such construction leads to multilayered models on  $3D$ -lattice, consisting of  $2D$  integrable planes-layers, with specific interaction between them. What is important is that transfer-matrix commutativity condition turns out to be not tetrahedron equation but an infinite set of usual Yang-Baxter equations. These equations can be satisfied simultaneously, producing the variety of  $3D$ -extended models [7] satisfying the necessary physical requirements — positivity of Boltzmann weights and locality of interactions.

Here we investigate the simplest example of such a model —  $3D$ -extended 6-vertex model, with the homogeneous set of interplane coupling constants. 6-vertex model is rather popular object to study, because of being limiting case for many solvable models in critical region (see e.g. [1]).  $3D$  solvable extension for 6-vertex model was obtained in [6] and in [7] generalized onto other solvable vertex models with charge conservation and inhomogeneous sequences of interplane interaction constants. In [6] the phase diagram for the free fermions case was conjectured. Here we go beyond this restriction and obtain the phase diagram in the general 3-parameter space, for the extended 6-vertex model.

The paper is organized as follows: first we remind the definition of the anisotropic  $3D$ -extended 6-vertex model and consider the strong interplane interaction limit. Then we give the

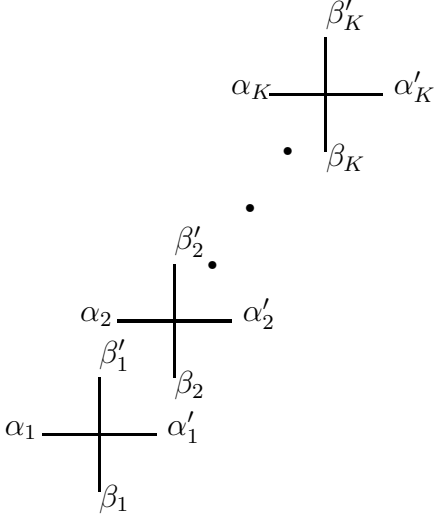


Figure 1: Multivertex consisting of  $K$  simple vertexes

alternative derivation of Bethe Ansatz (BA) equations, using the established gauge equivalence of our multilayer model to the set of  $2D$  6-vertex planes, each one in a field defined by the polarization of planes – neighbours. Using the symmetries of BA, we prove the equivalence between the model with homogenous set of interaction constants and some models with inhomogenous sets. We make use of these results, together with hypothesis of non-degeneracy of maximal eigenvalue, to eliminate the problem. The resulting phase diagram is obtained in the next section. Conclusion and discussing the possible generalizations closes the paper.

## 2 Definition of the model

The model we consider is system of  $K$  planes. Each of these planes is the symmetric 6-vertex solvable model on square  $N \times M$  lattice [9]. We can "paste" together  $ij$ -sites of all planes and formally get  $2D$  system with complex site consisting of  $K$  simple vertexes (see fig. 1).

Boltzmann weight of such multivertex fragment has form

$$\mathbf{L}_{\alpha'_1 \alpha'_2 \dots \alpha'_K \beta'_1 \beta'_2 \dots \beta'_K}^{\alpha_1 \alpha_2 \dots \alpha_K \beta_1 \beta_2 \dots \beta_K} = \prod_{k=1}^K L_{6v_{\alpha'_k, \beta'_k}}^{\alpha_k, \beta_k} \exp\{-h_k \alpha_k \beta_{k+1} + h_k \alpha'_{k+1} \beta'_k\} \quad (1)$$

where  $h_k$  are arbitrary constants, defining interaction between nearest neighbours in  $k$ -th and  $(k + 1)$ -th plane,  $L_{6v_{\alpha'_k, \beta'_k}}^{\alpha_k, \beta_k}$  — Boltzmann weights of "source" 6-vertex solvable model, state variables  $\alpha_k, \beta_k, \dots$  take values  $\pm 1$ . For the planes (layers) we impose periodic boundary conditions  $K + 1 \equiv 1$ . The permissible configurations of 6-vertex model are drawn on fig.2. The variables sitting on edges are represented by arrows on fig.2. "+" ("−") correspond to arrows pointing up or to the right (down or to the left). The local Boltzmann weights are invariant under inversion of all arrows.

### Strong interplane interaction limit $h \rightarrow \infty$ .

To understand the nature of interaction for the homogenous model (all interplane interaction constants  $h_k$  equal:  $h_k \equiv h$ , any  $k$ ), let us consider the strong interplane interaction limit

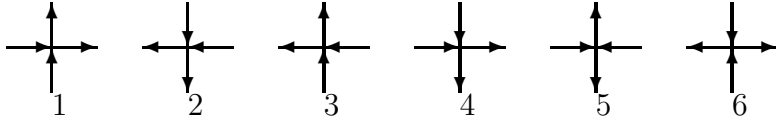


Figure 2: Fig.2. Permissible vertex configurations for 6-vertex model. Boltzmann weights of configurations:  $w_1 = w_2 = a$ ;  $w_3 = w_4 = b$ ;  $w_5 = w_6 = c$

$h \rightarrow \infty$ . The configuration with maximal Boltzmann weight will give the main contribution to the partition sum. To obtain this configuration, we should maximize exponential factor in (1) for all sites in all planes.

Without loss of generality, we can set  $\alpha_k = \beta'_k = +1$  for  $k$ -th plane. Then, to maximize the exponential factor in (1), we should choose  $\beta_{k+1} = -1$ ;  $\alpha'_{k+1} = +1$  in  $k + 1$ -th plane, i.e. vertex of type 4 (see fig.2), and  $\alpha_{k+1} = +1$ ;  $\beta'_{k+1} = -1$ . Performing the next step, we get  $\beta_{k+2} = \alpha'_{k+1} = -1$ . This fits vertexes of type 5 and 2; however vertex 5 is unsuitable<sup>1</sup>. Proceeding analogously further, we get: planes  $k - (k + 4)$  are formed by the vertexes of type 1, 4, 2, 3, 1, respectively. It is easy to see that each next vertex (next plane) can be obtained from the previous one by the clockwise rotation by  $\pi/2$ . After full rotation over  $2\pi$ , the configuration repeats.

Thus, in the strong interplane interaction limit, the model has homogenous structure within each horizontal plane, and spiral structure with period 4 in vertical direction: each next plane configuration is obtained from the previous one by clockwise  $\pi/2$  rotation:

$$\dots \nearrow \searrow \swarrow \nwarrow \dots \quad (2)$$

The arrows in formula above are the resulting from vector summation of all arrows in each plane: for example, the arrow  $\nearrow$  corresponds to homogenous configuration of vertexes of type 1 in Fig.2.

### 3 The matrix formulation

It is convenient to rewrite (1) in matrix form. Let us introduce  $2^{2K} \times 2^{2K}$  matrix  $\mathcal{L}^k$  acting in the tensor product  $\prod_1^K \otimes g_0 \prod_1^K \otimes g_n$  with elements

$$(\mathcal{L}^k)_{\alpha'_1 \alpha'_2 \dots \alpha'_K \beta'_1 \beta'_2 \dots \beta'_K}^{\alpha_1 \alpha_2 \dots \alpha_K \beta_1 \beta_2 \dots \beta_K} = \delta_{\alpha_1 \alpha'_1} \delta_{\beta_1 \beta'_1} \delta_{\alpha_2 \alpha'_2} \delta_{\beta_2 \beta'_2} \dots \delta_{\alpha_{k-1} \alpha'_{k-1}} \delta_{\beta_{k-1} \beta'_{k-1}} \exp(-h_k \alpha_k \beta_{k+1} + h_{k-1} \alpha'_k \beta'_{k-1}) \\ L_{6v}^{\alpha_k \beta_k}_{\alpha'_k \beta'_k} \delta_{\alpha_{k+1} \alpha'_{k+1}} \delta_{\beta_{k+1} \beta'_{k+1}} \dots \delta_{\alpha_K \alpha'_K} \delta_{\beta_K \beta'_K} \quad (3)$$

$L_{6v}$  is the  $4 \times 4$  local  $L$ -matrix of six-vertex model with the following nonzero elements:

$$L_{11}^{11} = L_{22}^{22} = a; \quad L_{12}^{12} = L_{21}^{21} = b; \quad L_{21}^{12} = L_{12}^{21} = c \quad (4)$$

in which  $a, b, c$  are Boltzmann weights of permissible configurations (see fig.2). Here and below in this section we borrow notations from paper of Faddeev and Takhtajan [5]. Note that

<sup>1</sup> In order to get maximal Boltzmann weight, we have to construct configuration in each plane with the same type of vertexes. This can be done with type-1 - 4 vertexes but not with type-5 vertexes -they always go in pairs with type 6 vertexes.

matrices  $\mathcal{L}^k$ , corresponding to neighbouring  $k$ -s, do not commute. The multivertex Boltzmann weights (1) are matrix elements of the ordered matrix product of  $\mathcal{L}^k$  over all planes:

$$\prod_{k=1}^K \mathcal{L}^k = \mathbf{L}$$

$$\mathbf{L}_{\alpha'_1 \alpha'_2 \dots \alpha'_K \beta'_1 \beta'_2 \dots \beta'_K}^{\alpha_1 \alpha_2 \dots \alpha_K \beta_1 \beta_2 \dots \beta_K} = \prod_{k=1}^K L_{6v \alpha'_k \beta'_k}^{\alpha_k \beta_k} \exp\{-h_k \alpha_k \beta_{k+1} + h_{k-1} \alpha'_k \beta'_{k-1}\} \quad (5)$$

(expressions (1) and (5) are the same, due to periodicity).

Using introduced notations we can write partition function of the model in usual (see e.g. [1]) form:

$$\mathbf{Z} = Tr(\mathbf{T})^M \quad (6)$$

with transfer-matrix  $\mathbf{T}$  being the trace of the ordered product of local matrices  $\mathbf{L}$  along the row (we'll denote matrix  $\mathbf{L}$  acting in the site  $n$  as  $\mathbf{L}_n$ ):

$$\mathbf{T} = Tr\left(\prod_{n=1}^N \mathbf{L}_n\right) \quad (7)$$

Here  $Tr$  operation and matrix product goes over  $\alpha$ -indexes (we'll call it: 'auxiliary' space) and  $Tr$  operation in the previous formula (6) goes over  $\beta$ -indexes ('quantum' space).

The free energy per site in the thermodynamic limit  $N, M, K \rightarrow \infty$  is defined by the maximal transfer-matrix eigenvalue

$$\mathbf{T}\Psi = \Lambda\Psi; \quad f = -k_B T \lim_{N, K \rightarrow \infty} \frac{1}{NK} |\Lambda_{max}|. \quad (8)$$

Important feature of our  $K$ -plane model is that its monodromy matrix  $\mathcal{T}$  can be written as an ordered product of more simple ones (we'll denote matrix  $\mathcal{L}^k$  from (3) acting in the site  $n$  as  $\mathcal{L}_n^k$ ):

$$\mathcal{T} = \prod_{n=1}^N \mathbf{L}_n = \prod_{n=1}^N \left(\prod_{k=1}^K \mathcal{L}_n^k\right) = \prod_{k=1}^K \left(\prod_{n=1}^N \mathcal{L}_n^k\right) = \prod_{k=1}^K \mathcal{T}_k \quad (9)$$

$$\mathcal{T}_k = \prod_{n=1}^N \mathcal{L}_n^k \quad (10)$$

Matrix  $\mathcal{L}^k$  from (3) can be written in compact form as can be easily verified:

$$\mathcal{L}^k = \exp(-h_k \sigma^{(k)} \tau^{(k+1)}) L_{6v}^k \exp(h_{k-1} \sigma^{(k)} \tau^{(k-1)}) \quad (11)$$

where we denote by the  $\sigma^{(k)}$  and  $\tau^{(k)}$  the diagonal matrix  $\sigma^z = \text{diag}(1, -1)$  acting nontrivially in  $k$ -th 'auxiliary' and  $k$ -th 'quantum' space, respectively:

$$\begin{aligned} (\sigma^{(k)})_{\alpha'_1 \alpha'_2 \dots \alpha'_K \beta'_1 \beta'_2 \dots \beta'_K}^{\alpha_1 \alpha_2 \dots \alpha_K \beta_1 \beta_2 \dots \beta_K} &= \delta_{\alpha_1 \alpha'_1} \dots \delta_{\alpha_{k-1} \alpha'_{k-1}} (\sigma^z)_{\alpha_k \alpha'_k} \delta_{\alpha_{k+1} \alpha'_{k+1}} \dots \delta_{\alpha_K \alpha'_K} \prod_{i=1}^K \delta_{\beta_i \beta'_i} \\ (\tau^{(k)})_{\alpha'_1 \alpha'_2 \dots \alpha'_K \beta'_1 \beta'_2 \dots \beta'_K}^{\alpha_1 \alpha_2 \dots \alpha_K \beta_1 \beta_2 \dots \beta_K} &= \delta_{\beta_1 \beta'_1} \dots \delta_{\beta_{k-1} \beta'_{k-1}} (\sigma^z)_{\beta_k \beta'_k} \delta_{\beta_{k+1} \beta'_{k+1}} \dots \delta_{\beta_K \beta'_K} \prod_{i=1}^K \delta_{\alpha_i \alpha'_i} \end{aligned} \quad (12)$$

## 4 Bethe Ansatz equations

It can be shown - see Appendix for a proof - that the 3D model under consideration (1) is gauge equivalent <sup>2</sup> to the set of 2D 6-vertex planes, each in its own horizontal field with the strength defined by the vertical polarization in neighbouring planes and interplane interaction constants:

for the  $k$ -th plane the field strength

$$H_k = h_k y_{k+1} - h_{k-1} y_{k-1} \quad (13)$$

where polarization  $y_k$  is defined as usual:

$$y_k = \frac{n_k^\uparrow - n_k^\downarrow}{n_k^\uparrow + n_k^\downarrow} = \frac{2n_k^\uparrow - N}{N} \quad (14)$$

$n_k^\uparrow$  ( $n_k^\downarrow$ ) is the number of upward (downward) pointing arrows in horizontal row in plane  $k$ .

Therefore, the Bethe Ansatz of the model is given by the well-known formulas for 6-vertex model in an external horizontal field (see e.g. [9]); below  $n_k = n_k^\uparrow$ ,  $y_k = \frac{2n_k - N}{N}$ :

$$\Lambda_k(H_k) = a^N e^{NH_k} \prod_{j=1}^{n_k} \frac{a\tau_j^{(k)} - b(2\Delta\tau_j^{(k)} - 1)}{a - b\tau_j^{(k)}} + b^N e^{-NH_k} \prod_{j=1}^{n_k} \frac{b - a(2\Delta - \tau_j^{(k)})}{-a + b\tau_j^{(k)}} \quad (15)$$

where  $\tau_j^{(k)}$  satisfy the set of Bethe Ansatz equations

$$e^{2NH_k} (\tau_j^{(k)})^N = (-1)^{n_k+1} \prod_{l=1}^{n_k} \frac{\tau_j^{(k)} \tau_l^{(k)} - 2\Delta\tau_j^{(k)} + 1}{\tau_j^{(k)} \tau_l^{(k)} - 2\Delta\tau_l^{(k)} + 1} \quad (16)$$

$$n_k = 1, 2, \dots, N; \quad k = 1, 2, \dots, K$$

where

$$\Delta = \frac{a^2 + b^2 - c^2}{2ab} \quad (17)$$

$a, b, c$  are Boltzmann weights of symmetrical 6-vertex model configurations (see fig.2).

The global transfer-matrix eigen-value is the product of those over all planes:

$$\Lambda_{\{h\}}^{\{y\}} = \Lambda_{y_1}^{h_1} \Lambda_{y_2 \dots y_K}^{h_2 \dots h_K} = \Lambda_{y_1}(H_1) \Lambda_{y_2}(H_2) \dots \Lambda_{y_K}(H_K); \quad y_p = \frac{2n_p - N}{N} \quad (18)$$

The Eqs. (15,16) were obtained directly in [6, 7] using the quantum inverse scattering method, and the analytic ansatz method, respectively.

We shall restrict ourselves to the model with all interplane interaction constants equal:  $h_k \equiv h$ , any  $k$  (below we refer to that case as to the homogenous model). However as is shown below, our results are valid also for some models with inhomogenous sequences  $\{h_k\}$ .

To obtain the bulk free energy and complete phase diagram, one should find such a sequence of  $n_k$ ,  $\{n_k\}_{k=1}^K$  that corresponds to the maximal transfer-matrix eigen-value  $\Lambda_{max}$ , and  $\Lambda_{max}$  itself, in complete 3-parameter space  $a/c$ ,  $b/c$ ,  $h$ . This program can be performed easily in the following limiting cases:

---

<sup>2</sup>We thank Yury Stroganov for drawing our attention to this fact

1) for the single 6-vertex model (decoupled planes limit  $h = 0$ ). Then BA solutions  $\tau_i^{(k)}$  lie on a unit circle  $\tau_j^{(k)} = e^{i\lambda_j^{(k)}}$ ,  $\lambda_j^{(k)}$  real. The expression for  $\Lambda_{max}$  is found then by the integral equation method (see e.g. [1]).

2) 'Ising chain' case  $\Delta = \pm\infty$ , i.e.  $a = 0$  or  $b = 0$ , any  $h$  is equivalent to  $\Delta = \pm\infty$ ,  $h = 0$ . Thus it is reduced to the previous case.

3) for the free fermions case  $\Delta = 0$ . Then RHS of (16) is equal to 1, and BA is solved trivially. The complete analysis is done in [6].

In the general case i.e. nonzero  $h$  and  $\Delta$ , the structure of BA equations doesn't permit simple analysis. The reason is in that case the locus of BA roots is unknown. The problem is similar to that arising when one considers usual 6-vertex model in external horizontal field (see [9, 1]).

### Connections between models with interplane constants

$\{\dots h, h, h, h, \dots\}$ ,  $\{\dots h, -h, h, -h, \dots\}$ , and arbitrary sets of 'h' and '-h'.

The models listed in the title look different, and different they are, having for instance, different 'strong interplane interaction limit'  $h \rightarrow \infty$  (this can be verified directly as it was done for homogenous model at the beginning of the paper). We'll show however that they have precisely the same transfer-matrix spectrum, and therefore the same phase diagram, with minor redefinition of phases.

Let us take the state of the  $k$ -th plane with  $n_k$  arrows pointing up, in a field  $H_k$ , described by Eqs. (15,16). Reversing of all horizontal and vertical arrows, together with changing the sign of  $H_k$ , leaves the Boltzmann weights and therefore the eigen-value (15) invariant:

$$\Lambda_{y_k}(H_k) = \Lambda_{-y_k}(-H_k) \quad (19)$$

(Bethe Ansatz (16) changes accordingly). Using this formula, write the global transfer-matrix eigenvalue (18) for the set  $\{y_1, y_2, -y_3, -y_4, y_5, y_6, -y_7, -y_8, \dots -y_K\}$  for the homogenous model:

$$\Lambda_{y_1}^h \Lambda_{y_2}^h \Lambda_{-y_3}^h \Lambda_{-y_4}^h = \Lambda_{y_1}(h(y_2 + y_K)) \Lambda_{y_2}(h(-y_3 - y_1)) \Lambda_{-y_3}(h(-y_4 - y_2)) \Lambda_{-y_4}(h(y_5 + y_3)) = \Lambda_{y_1}(h(y_2 + y_K)) \Lambda_{y_2}(h(-y_3 - y_1)) \Lambda_{y_3}(h(y_4 + y_2)) \Lambda_{y_4}(h(-y_5 - y_3)) \quad (20)$$

**Remark.** Here and below we assume the number of planes  $K$  to be infinitely large and divisible by all numbers  $K = 2 * 3 * 4 * \dots$ ,  $K + 1 \equiv 1$ , to avoid complications connected with the boundary effects. For the sake of simplicity we write down only the significant part of the multiplication (18), then it continues periodically.

Let us write down the global eigenvalue for the system with alternating constants:

$$\Lambda_{y_1}^h \Lambda_{y_2}^{-h} \Lambda_{y_3}^h \Lambda_{y_4}^{-h} = \Lambda_{y_1}(h(y_2 + y_K)) \Lambda_{y_2}(h(-y_3 - y_1)) \Lambda_{y_3}(h(y_4 + y_2)) \Lambda_{y_4}(h(-y_5 - y_3)) \quad (21)$$

Comparing with the previous formula we have

$$\Lambda_{y_1}^h \Lambda_{y_2}^h \Lambda_{-y_3}^h \Lambda_{-y_4}^h = \Lambda_{y_1}^h \Lambda_{y_2}^{-h} \Lambda_{y_3}^h \Lambda_{y_4}^{-h} \quad (22)$$

(periodical continuation is implied - see Remark above).

Analogously one obtains

$$\Lambda_{y_1}^h \Lambda_{y_2}^h \Lambda_{y_3}^h \Lambda_{y_4}^h = \Lambda_{y_1}^h \Lambda_{y_2}^h \Lambda_{y_3}^{-h} \Lambda_{y_4}^{-h} \quad (23)$$

Actually, one could coin such transformations between the model with homogenous sequences and those with arbitrary sequences of 'h' and '-h':  $\{h_k\}_{k=1}^K$ ,  $h_k = \pm 1$ ,  $k = 1, 2, \dots K$ . For instance,

$$\Lambda_{y_1 y_2 y_3}^{h h -h} = \Lambda_{y_1 y_2 y_3 -y_4 -y_5 -y_6}^{h h h \dots \dots h} \quad (24)$$

and so on.

## 5 Symmetries

Here we make use of the results of previous paragraph to establish transformations which map the eigenvalue to the eigenvalue of the same model.

First of all, note that simultaneous inversion of polarization in all planes  $Z$

$$Z\{y\} = \{-y\} \quad (25)$$

leaves the eigenvalue invariant:

$$\Lambda_{\{-y\}}^{\{h\}} = \prod_k \Lambda_{-y_k}^{h_k} (-h_k y_{k+1} + h_{k-1} y_{k-1}) = \prod_k \Lambda_{y_k}^{h_k} (h_k y_{k+1} - h_{k-1} y_{k-1}) = \Lambda_{\{y\}}^{\{h\}}$$

This is also the direct consequence of the fact that local Boltzmann weight (1) is invariant under transformation *all*  $\alpha_k, \beta_k \rightarrow -\alpha_k, -\beta_k$ .

Another transformation we obtain, inverting the order of  $\{y\}$ -set and  $\{-h\}$ -set:

$$\Lambda_{y_1 y_2 \dots y_K}^{h_1 h_2 \dots h_K} = \Lambda_{y_1 y_K y_{K-1} \dots y_3 y_2}^{-h_K -h_{K-1} \dots -h_2 -h_1}$$

(this is proved analogously) Transformation J

$$J\{y_1 y_2 \dots y_K\} = \{y_1 y_K y_{K-1} \dots y_3 y_2\} \quad (26)$$

is a symmetry for the model with alternating constants:

$$\Lambda_{\{y\}}^{h -h h -h} = \Lambda_{J\{y\}}^{h -h h -h}$$

Then, one more independent symmetry exist for that model:

$$F\{y\} = \{y_2 -y_3 \dots y_K -y_1\}; \quad \Lambda_{\{y\}}^{h -h h -h} = \Lambda_{F\{y\}}^{h -h h -h} \quad (27)$$

For completeness, we define operator of one-step shifting  $S$ :

$$S\{y\} = \{y_2 y_3 \dots y_K y_1\} \quad (28)$$

Evidently,  $S^n$ , integer  $n$ , is a trivial symmetry for the homogenous model and  $S^{2n}$  is a trivial symmetry for the model with alternating constants. Transformations  $Z, J, F, S^2$  are basic symmetries for the model with alternating constants. Let us obtain the basic symmetries for the homogenous case.  $Z$  and  $S$  are the symmetries already.

Then, define the transformation from (22) between the two models:

$$Q\{y\} = \{y_1 y_2 -y_3 -y_4 \dots\}; \quad Q^{-1} = Q$$

Transformations  $QJQ$  and  $QFQ$  are the symmetries sought for:

$$P\{y\} = QJQ\{y\} = \{y_1 -y_K y_{K-1} -y_{K-2} \dots y_3 -y_2\}; \quad P^2 = I \quad (29)$$



$$QFQ = S$$

So, for the homogenous model *all*  $h_k \equiv h$  two nontrivial symmetries  $Z$  and  $P$  exist defined by the (25),(29). Working out the same procedure for the model  $h, h, -h, -h \dots$  doesn't give additional information. It is noteworthy also that the  $Z$ -symmetry is not independent but can be expressed in terms of shifting and  $P$ -symmetry

$$Z = (SP)^2$$

Nevertheless it proves convenient to keep it in mind as a separate symmetry. As is shown below,  $Z$  and  $P$  symmetries, having been combined with the non-degeneracy hypothesis, put drastic constraints on the polarization set  $\{y\}$  which corresponds to the maximal eigenvalue of the global transfer-matrix of the homogenous model.

## 6 Finding the maximal eigenvalue set $\{y\}$

We are now in a position to solve the maximal eigenvalue problem, for the homogenous model. First we have to point out which set  $\{y\}$  corresponds to it for any value of parameters  $a/c, b/c, h$ . We shall parametrize the possible sets by a period  $T$  and define the set  $\{y^{(T)}\}$  as that with periodically repeating entries:

$$\{y^{(T)}\} = \{y_1 y_2 \dots y_T y_1 y_2 \dots y_T \dots y_T\}; \quad \{y^{(T)}\}_{T+n} = \{y^{(T)}\}_n$$

Note that cases  $T = 1$  and  $T = 2$  are trivial because they lead to vanishing of interaction  $h$  from all expressions (see (13)– (16)). The symmetry  $Z$  (see (25)) does not effect the period  $T$  of the set, but the symmetry (29) does. Having been applied for odd  $T = 2n + 1$ , it doubles the period:

$$P\{y^{(T)}\} = \{\tilde{y}^{(2T)}\} \tag{30}$$

For instance for the period  $T = 3$

$$P\{y_1 y_2 y_3 \dots\} = \{y_1 -y_3 y_2 -y_1 y_3 -y_2 \dots\}$$

(We write down only the simplest periodically repeating pattern).

Note that set  $\{y^{(T)}\}$ , *odd*  $T$  for the homogenous model, corresponds to the sequence of period  $4T$  for the model with alternating constants:  $Q\{y^{(T)}\} = \{\tilde{y}^{(4T)}\}$

For the sets with even  $T = 2n$  the symmetry (29), generally speaking, does not effect the period, as can be easily verified.

To go further, we need an additional piece of information concerning the maximal eigenvalue set  $\{y\}$ . We supply it by stating:

*The maximal eigen-value set for the homogenous model is unique, modulo shift, for all phases except the ferroelectric phase I (see fig.3).*

This statement is equal to stating that maximal global transfer matrix eigenvalue is non-degenerate. For the 'source' 6-vertex model, this is true:  $y = 0$  for all phases except ferroelectric, and  $y = 0$  is just the value invariant under action of  $Z$ -symmetry (25). Strong coupling limit  $h \rightarrow \infty$  is non-degenerated, too. As to the exclusion - ferroelectric phase I (see fig.3), it has degeneracy  $2^K$ ,  $K$  being the number of planes. Indeed the ferroelectric phase is built up from  $a$ - (or  $b$ -) vertexes only. It follows from (1) that Boltzmann weight does not depend on  $h$  for the homogenous model, whatever  $a$ -vertexes (type 1 or type 2 -see fig.2) form each plane.

For all other phases, the hypothesis of non-degeneracy means that the maximal set  $\{y\}_{max}$  is invariant under action of  $Z$ - and  $P$ -symmetries (25,29), modulo arbitrary shift <sup>3</sup>

The immediate consequences are:

1) from the (25): that the average value of  $\langle y_p \rangle_{max}$  must be zero:

$$\frac{1}{K} \sum_{p=1}^K y_p = 0$$

2) from the (30): that the maximal set cannot have an odd period.

The period of maximal set also cannot be  $T = 2n$ ,  $n$  odd. To see that, consider  $T = 6$ . For the set to be invariant under action of  $Z$ -symmetry (25) it must have form

$$\{y^{(6)}\} = \{u v w -u -v -w \dots\}$$

Acting on it by the  $P$ -symmetry

$$P\{y^{(6)}\} = \{u w -v \dots\},$$

one obtains the set with period 3. Analogously one obtains  $P\{y^{(2n)}\} = \{\tilde{y}^{(n)}\}$ ,  $n$  odd, in contradiction with non- degeneracy hypothesis.

Since the maximal sets  $\{y^{(T)}\}$  with  $T$  and  $T/2$  odd are forbidden, we are left with the only possible choice

$$T = 4n$$

For that case,  $P\{y^{(4n)}\} = \{\tilde{y}^{(4n)}\}$  always.

The first nontrivial case is  $T = 4$ . Note that it is just the period which arises in the strong interplane interaction limit  $h \rightarrow \infty$ . According to  $Z$ -symmetry (or as well to  $P$ -symmetry) invariance, the maximal set reads

$$\{y^{(4)}\} = \{\eta \xi -\eta -\xi \dots\} \quad (31)$$

$T = 8$ .  $P$ - and  $Z$ -symmetry invariance lead to the following set:

$$\{y^{(8)}\} = \{u v 0. v -u -v 0. -v \dots\} \quad (32)$$

With increasing  $T$ , admissible structure looks more and more complicated. For  $T = 12$

$$\{y^{(12)}\} = \{u v w r -w v -u -v -w -r w -v \dots\} \quad (33)$$

and so on. Thus, we have produced the hierarchy of sequences which are candidates for the planes polarization set  $\{y\}_{max}$  corresponding to the maximal global transfer-matrix eigenvalue. The number of parameters is reduced essentially but still there is quite a freedom left. The results are in agreement with numerical data. The latter however forces us to formulate the final hypothesis which we cannot prove. It is described in the section to follow

## 7 The final hierarchy

Let us assume that the maximal set contains at least one plane  $k$  with maximal polarization  $y_k = 1$ . It follows immediately from (25) and non-degeneracy, that some another plane  $p$  has

<sup>3</sup> Note that for the model with alternating constants  $\{\dots h, -h, h, -h, \dots\}$ , the maximal set  $\{y\}_{max}$  is always degenerate. It is the additional symmetry  $F$  (27) that accounts for the degeneracy. The same holds for the model with the constants  $\{\dots h, h, -h, -h, \dots\}$ .

$y_p = -1$ . Denote the distance between these two planes by  $A = |p - k|$ . We shall parametrize the sequences  $\{y\}$  by the value of  $A$ . The entries of maximal set  $\{y\}_{max}$  obey the following rule:

$$\left. \begin{aligned} y_{k+n} &= -y_{k-n}, & n \text{ odd} \\ y_{k+m} &= y_{k-m}, & m \text{ even} \end{aligned} \right] \quad (34)$$

and the same with the replacement of  $k$  by any other number  $\tilde{k}$ , where  $y_{\tilde{k}} = \pm 1$ . From (34) those numbers are  $\tilde{k} = k \pm An$ , *integer*  $n$ . Making use of (34), for  $A$  odd we obtain the  $y$ -set of period  $4A$   $\{y^{(4A)}\}$ , and  $\{y^{(2A)}\}$ , for  $A$  even. The rules (34) are consistent with  $Z$  and  $P$  symmetries, and can be derived from them.

Let us take  $A = 1$ . Here we have

$$\{y\} = \{1 \ 1 \ -1 \ -1 \ \dots\} \quad (35)$$

— just the maximal set for the  $h \rightarrow \infty$  limit (phase 4 in the phase diagram).  $A = 2$  produces the set

$$\{y\} = \{1 \ -\xi \ -1 \ \xi \ \dots\} \quad (36)$$

- the maximal set for the phase 5 in the phase diagram. It coincides with that from (32) when  $\eta = 1$ . For  $A = 3$  one obtains from Eqs. (34):

$$\{y\} = \{1 \ v \ w \ -1 \ -w \ v \ -1 \ -v \ -w \ 1 \ w \ -v \ \dots\} \quad (37)$$

which coincides with (33) when  $u = 1$ ,  $r = -1$ .

$A = 4$  produces the set (32) with the substitution  $u = 1$ , and so on.

Phases with  $A = 1, 2$  do exist on the phase diagram. However we have failed to find there numerically the phases with  $A = 3, 4$ . From that we conclude that another members of hierarchy, with  $A > 4$  don't appear, too. We suggest that the higher members of hierarchy do appear when one includes into consideration more distant than nearest neighbours, plane-plane interaction. For instance, we have checked that the phase with  $A = 3$  (37) does enter the phase diagram when one includes additional interaction between the planes  $k \rightarrow k + 3$ , *any*  $k$ .

## 8 The phase diagram

We have shown in the last two sections that the set of polarization constants  $\{y\} = y_1 \ y_2 \ \dots \ y_K$  which corresponds to the maximal eigenvalue (the maximal set) must have the period divisible by 4:  $T = 4n$ . For the simplest case  $T = 4$  the maximal set is (31) and the transfer-matrix eigenvalue is given by Eq.(20), with the substitution  $y_1 = y_3 = y_5 = \eta$ ;  $y_2 = y_4 = y_K = \xi$

$$\Lambda^{2/K} = \Lambda_\eta(2h\xi)\Lambda_\xi(-2h\eta)$$

We can always choose  $\xi$  and  $\eta$  positive. Therefore we only have to maximize the eigenvalue (18) within the two-parameter space

$$\xi = \frac{2n - N}{N}; \quad \eta = \frac{2m - N}{N}; \quad n, m = 0, 1 \dots \frac{N}{2}$$

By means of the Newton-Ralphson method we are able to solve BA equations directly and find the block with largest eigen-value for system size up to  $N = 32$ .

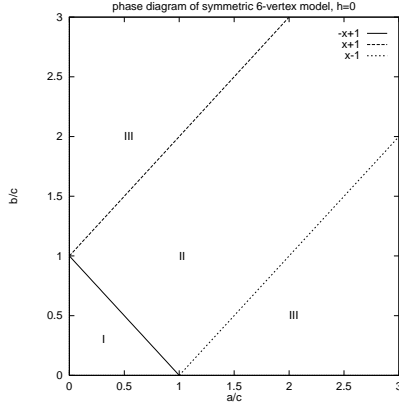


Figure 3: Phase diagram of the 2D 6-vertex model (corresponds to decoupled planes limit  $h = 0$ )

It turns out however that the maximal eigen-value for all values of parameters  $a, b, c$  and  $h$  belongs either to the block  $n = m = N/2$  (in that case  $h$  vanishes from all equations (15,16), yielding the known results for 6-vertex model), or to the block with at least one of  $n, m$ , say  $m$  equal to zero:  $m = 0$ . Finally the Bethe Ansatz (15,16) rewritten

$$\begin{aligned} \Lambda^{2/K} &= \Lambda_{m=0}(2h\xi)\Lambda_\xi(2h) = \Lambda_1\Lambda_2 \\ \Lambda_1 &= a^N e^{2h(2n-N)} + b^N e^{-2h(2n-N)} \\ \Lambda_2 &= a^N e^{2hN} \prod_{j=1}^n \frac{a\tau_j - b(2\Delta\tau_j - 1)}{a - b\tau_j} + b^N e^{-2hN} \prod_{j=1}^n \frac{b - a(2\Delta - \tau_j)}{-a + b\tau_j} \\ e^{4hN} (\tau_j)^N &= (-1)^{n+1} \prod_{l=1}^n \frac{\tau_j\tau_l - 2\Delta\tau_j + 1}{\tau_j\tau_l - 2\Delta\tau_l + 1} \end{aligned}$$

Note that the eigen-value is invariant under the transformation:

$$a \rightarrow b, \quad b \rightarrow a, \quad h \rightarrow -h$$

Figures 3-6 show the phase diagram of the model in the space of Boltzmann weights ratios  $a/c, b/c$ , for the different values of interplane constant  $h$ . Fig.3 (decoupled planes,  $h=0$ ) repeats well-known results for usual 6-vertex model: the three distinct phases exist separated by the lines  $\Delta = \pm 1$ . These phases are (for details see [9]):

I. Antiferroelectric phase. C-Vertexes (type 5 and 6) are dominant; In sufficiently low temperatures vertex plane configuration is filled with arrows alternating in both directions with step 1.

II. Disordered phase  $-1 < \Delta < 1$ . All types of vertexes are present; there are no types of vertexes which are dominant. Here lies the high temperature limit so one should expect disorder.

III. Ferroelectric phase  $\Delta > 1$ . Phase III occupies two separated regions, the left upper and the right bottom in the phase diagram. In the left upper region,  $b/c > a/c + 1$ , each plane is occupied by either exclusively type 3, or exclusively type 4 vertexes. It is convenient to consider the arrow resulting from vector summation of all arrows in the plane:

for the type 3 configuration, all arrows on the plane are pointing up and to the left, resulting is upleft arrow  $\nwarrow$ , whereas for the type 4 configuration, the resulting is downright arrow  $\searrow$ ,

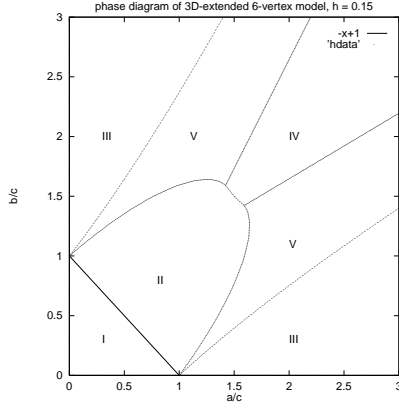


Figure 4: Phase diagrams of the 3D-extended 6-vertex model on cubic lattice in the  $a/c$ ,  $b/c$  plane,  $h = 0.15$ . The phase transitions between the phases II/IV, II/V, V/III are of the first order. The phase transitions between the phases IV/V are of the second order, Pokrovsky-Talapov type. Transition I/II is the Kosterlitz - Thouless type transition. Curves separating phases III/V , V/IV) are given by:  $\Delta = \cosh 4h$  ( $b/c = (a/c) \exp 4h - 1$ ), respectively.

see Fig.2. Polarization vector (14) modulus reaches its maximum  $|y| = 1$ , namely,  $y = 1$  for the type 3 configuration and  $y = -1$  for the type 4 configuration.

If we associate with the each plane  $k$  the corresponding arrow —  $\nwarrow$  for type 3,  $\searrow$  for type 4 configuration, then the state of the multiplane model in phase III, left upper region, is characterized by the random sequence

$$\dots \nwarrow \searrow \searrow \nwarrow \searrow \nwarrow \nwarrow \nwarrow \dots \tag{38}$$

consisting of these arrows randomly placed. Of course switching on some vanishing external field favouring type 3 configuration will lift up this degeneracy, giving the homogenous sequence:

$$\dots \nwarrow \nwarrow \nwarrow \nwarrow \nwarrow \nwarrow \nwarrow \dots$$

The state of the model in the right bottom region, phase III,  $a/c > b/c + 1$  will be analogously characterized by the type 1, type 2 vertexes configurations, or upright, downleft  $\nearrow$ ,  $\swarrow$  arrows.

$$\dots \nearrow \nearrow \nearrow \swarrow \nearrow \swarrow \swarrow \nearrow \dots$$

In Fig.4- 6 the phase diagrams for the systems with a fixed  $h$  in increasing order are given. The phases I - III are exactly the same as in uncoupled planes limit in Fig.3. For nonzero coupling  $h$  the regions occupied by the phase III are given by the formula  $\Delta = \cosh 4h$ , and two new phases arise.

V. Layered antiferroelectric phase. This phase is exactly the one described as the strong interplane coupling limit in section 2. Each plane is in ferroelectric phase, but plane  $k + 1$  configuration strictly follows from one in  $k$ -th plane by  $\pi/2$  clockwise rotation. So, the planes-layers in increasing order are formed by the unique, up to shifting, sequence of vertexes, or resulting arrows:

$$\dots \nearrow \searrow \swarrow \nwarrow \nearrow \searrow \swarrow \nwarrow \dots$$

(compare with the sequence (38)).

In that phase polarization vector (14) alternates each other plane  $y_{k+2} = -y_k$ :

$$\dots y_k, y_{k+1}, \dots = \dots 1; -1; -1; 1; 1; -1; -1; 1 \dots \tag{39}$$

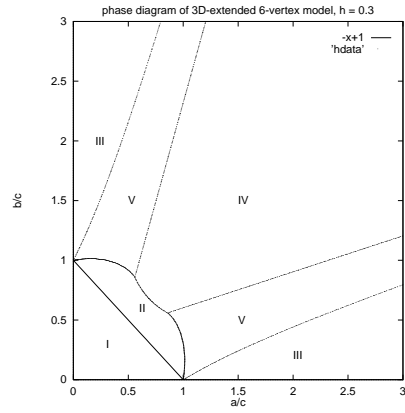


Figure 5: Phase diagram of the 3D-extended 6-vertex model on cubic lattice in the  $a/c$ ,  $b/c$  plane,  $h = 0.3$

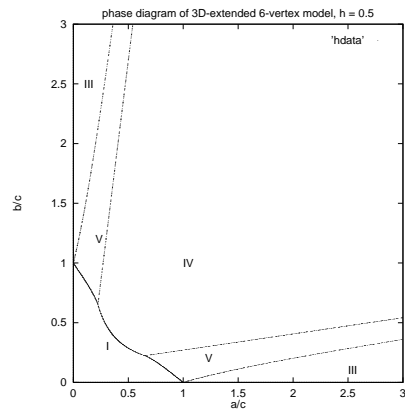


Figure 6: Phase diagram of the 3D-extended 6-vertex model on cubic lattice in the  $a/c$ ,  $b/c$  plane,  $h = 0.5$

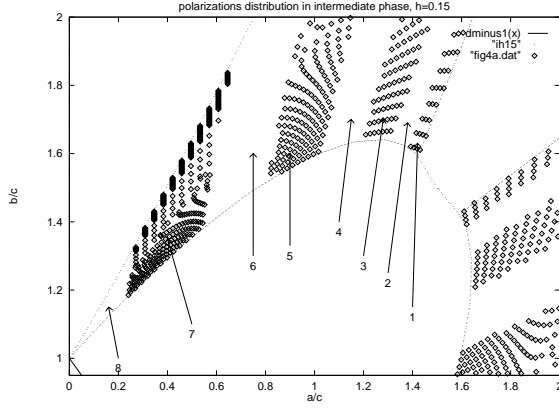


Figure 7: Distribution of polarizations in the intermediate phase V.  $h=0.15$ . This phase is characterized by the periodically repeated set of polarizations (in planes) (36)  $\{1 -\xi -1 \xi \dots\}$ ,  $\xi = (2n - N)/N$ ,  $n$  being the number of upward pointing arrows in a row in the corresponding plane. The results of numerical calculations of  $\xi$  for the system size  $N = 32$  are shown. The area is divided into 8 sectors, sector number  $k$  corresponds to  $2k - 1 \leq n \leq 2k$ . Thus, polarization monotonically increases from  $\xi = -1$  on the second order phase transitions line to  $\xi = 0$  near the point  $(0,1)$ . On the 'free fermions' circle  $\Delta = 0$  inside the intermediate phase, exact value of  $\xi$  is given by  $\sin(\pi\xi/2) = -(a/b)\sinh(4h)$ .

forming the layered antiferroelectric structure (in each separate plane the structure is ferroelectric) Polarization vector modulus in each plane reaches its maximal value  $|y_k| = 1$ , any  $k$ .

V. Phase V is an intermediate phase which can be described as follows: system splits into two subsystems, each contains two planes  $k$ -th and  $(k + 2)$ -th, e.g. (the first and the third) and (the second and the fourth). In one of the subsystems the planes are in ferroelectric phase, with alternating polarization vector  $y_k = 1$ ,  $y_{k+2} = -1$ . Another subsystem is partially disordered  $y_{k+1} = 2x - 1 = -y_{k+3}$ . Again as the previous one, this structure has period 4. Within the phase 4,  $x$  varies (see Fig. 4a,b); on transition line between phases IV/V  $x$  goes to zero continuously, forming the strong interplane coupling structure in phase 4. For the free fermions limit,  $\Delta = 0$ , or  $a^2 + b^2 = c^2$ , value of  $x$  is known exactly (see [6])

$$\cos \pi x = \frac{a}{b} \sinh 4h, \quad \text{for } a < b \quad (40)$$

Outside the free fermions curve, the branches with equal polarizations are arranged quite regular, as is seen from Fig.7,8. However we cannot present the exact formula for the moment.

The analytical and numerical calculations show that there are no other phases at the phase diagram.

The second order phase transition between the phases V/IV can be found considering the equality

$$\Lambda(n/N \rightarrow 0) = 1 \quad (41)$$

. Proceeding analogously as in [9] we get

$$\tau_j = e^{-4h}$$

. For  $ae^{4h} > b, b > a$  we have

$$\prod \frac{a\tau_j - b(2\Delta\tau_j - 1)}{a - b\tau_j} e^{-4h} = \prod \frac{a - 2b\Delta + be^{4h}}{ae^{4h} - b} e^{-4h} = 1$$

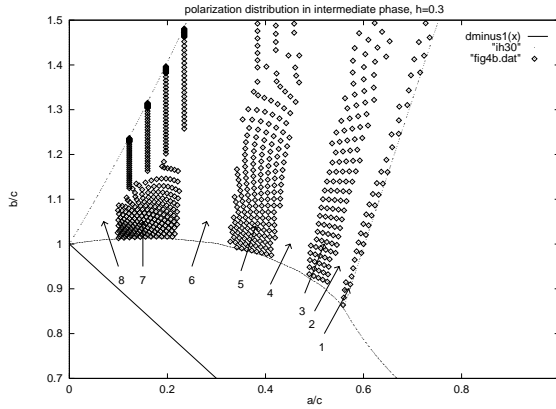


Figure 8: Distribution of polarizations in the intermediate phase V.  $h=0.3$ .

and  $\frac{a}{b} \sinh 4h = 1 - \Delta e^{-4h}$ , or using (17),

$$b/c = (a/c) \exp(4h) - 1 \quad (42)$$

All phase curves are symmetrical with respect to  $a = b$  line.

Proceeding with the same equality (41) and taking  $b > ae^{4h}$ , we obtain:

$$\Delta = \cosh 4h \quad (43)$$

But now this line marks only right margin for the phase transition III/V, and not necessarily the exact point. We have found however with all numerical accuracy that line (43) is exact transition point indeed. With increasing  $h$ , the phases IV and V expand in space, and the others diminish. When  $h$  reaches  $h_1 = 0.458134\dots$  and higher, phase II disappears completely as is shown in Fig.6. The fraction of space occupying by the phases II,III, diminishes exponentially with  $h$ , as is seen from (42, 43).

Finally, the transition line between the phases II/IV (II/V) or I/IV (I/V) in Fig.4-6 is obtained numerically. The line ends in points (0,1) and (1,0) which agrees with the limiting 'Ising chain' case. Phase transition II/IV (II/V) or I/IV (I/V) is of first order. Indeed in phases II or I the partition sum does not depend on  $h$  at all; (all  $n_k \equiv N/2$  and polarization vector  $y_k$  for all  $k$  is zero. The values of  $y_k$ -set jump when crossing the critical curve and dependence on  $h$  shows up. So the partition sum will have a cusp as a function of  $h$ .

The transition IV/V is of the second order. On this line, the order parameters — polarization vectors  $y_k$  (14) change continuously when approaching the critical point. The second derivative for free energy over  $h$  diverges as inverse square root  $\sim 1/\sqrt{h - h^*}$  in the critical point (Pokrovsky-Talapov type transition [10]).

We have described the phase diagram of the 3D-extended model with the homogenous set of constants. The phase diagrams for the models with arbitrary sets of ' $h$ ' and ' $-h$ ' constants are the same, with redefinition of phases (see Eqs.(22-24)). Note that for the model with alternating constants,  $\{\dots h, -h, h, -h, \dots\}$ , the period is always 2 (in planes).



## Conclusion

We have obtained the phase diagram for 3D solvable multilayered 6-vertex model, in full 3-parameter space. The model enjoys locality of interactions and positivity of Boltzmann weights. The applicability of the method to other solvable vertex models with ice rule (46) is shown in [7]. in view of possible applications, note that the strength of layer- layer interaction  $h$  can vary from plane to plane, as well as anisotropy parameter within each layer. Another possibility is to include more distant than nearest neighbour, interactions along 3-rd axis. The resulting solvable models are ones with competing interactions [8].

Another interesting question is the universality class of the model we have considered. The finite size scaling analysis (see e.g.[11]) of new (due to plane-plane coupling) critical phase, named V in the phase diagram, shows that it is described by 2D conformal field theory with central charge  $c = 1$ . Thus it belongs to the same universality class as the "source" 6-vertex model.

## Acknowledgements

One of the authors (VP) thanks colleagues from the Institute for Theoretical Physics, University of Amsterdam, where this work was mainly done, for the hospitality, and Prof. Doochul Kim for nice introduction to finite size scaling. This work was supported in part by the INTAS grants 93 – 1324, 93 – 0633, Soros grant K5Z100 and by the Erwin Shrödinger Institute, Vienna. This work was supported in part by the Korea Science and Engineering Foundation through the SRC program. We thank referees for good comments.

## Appendix

The partition function for the system with open boundaries is given by

$$\mathbf{Z} = \mathcal{T}^M$$

where  $\mathcal{T}$  is the global monodromy matrix. In our case (see Eqs. (3– 11))  $\mathcal{T}$  factorizes into product

$$\mathcal{T} = \prod_{k=1}^K \mathcal{T}_k \tag{44}$$

where the 'local monodromy matrix' for the  $k$ -th plane

$$\mathcal{T}_k = \prod_{n=1}^N e^{-h_k \sigma^{(k)} \tau_n^{(k+1)}} L_n^{(k)} e^{h_{k-1} \sigma^{(k)} \tau_n^{(k-1)}}$$

$L_n$  being the matrix of Boltzmann weights for the 6-vertex model, upper index ( $k$ ) corresponds to the  $k$ -th plane, matrices  $\sigma$  and  $\tau$  are defined by (12). Omitting the index  $k$  in the right-hand side of the last formula for convenience and denoting

$$\sigma^{(k)} \rightarrow \sigma; \quad \tau_n^{(k+1)}, \tau_n^{(k-1)} \rightarrow \tau'_n, \tau''_n, \quad h_k \rightarrow h, \quad h_{k-1} \rightarrow g,$$

we have:

$$\mathcal{T}_k(h, g) = \prod_{n=1}^N e^{-h\sigma\tau'_n} L_n e^{g\sigma\tau''_n} = e^{-h\sigma\tau'_1} L_1 e^{g\sigma\tau''_1} e^{-h\sigma\tau'_2} L_2 e^{g\sigma\tau''_2} \dots e^{-h\sigma\tau'_N} L_N e^{g\sigma\tau''_N} \quad (45)$$

The exponential factors in this expression commute with each other because they are diagonal matrices (see (12)). The commutation with  $L_n$  is given by

$$[\exp(h(\sigma + \tau_n)\tau''_p), L_n] = [\exp(h(\sigma + \tau_n)\tau'_p), L_n] = 0;$$

which is equivalent [6, 7] to the charge conservation property of the "source" 6-vertex model (4):

$$L_{6v_{\alpha'\beta'}}^{\alpha\beta} = 0, \quad \text{unless } \alpha' + \beta' = \alpha + \beta \quad (46)$$

Using these commutation rules, we move all exponents in (45) outside to the left and to the right. For instance, to move the term  $e^{-h\sigma\tau'_2}$  to the left, one inputs unity

$$e^{-h\sigma\tau'_2} e^{\pm h\tau_1\tau'_2} = e^{-h(\sigma+\tau_1)\tau'_2} e^{h\tau_1\tau'_2}$$

The first factor in this expression commutes with  $L_1$  and goes to the left while the second one commutes with all  $L_1, L_2, \dots, L_N$  (because they act in the different subspaces) and goes to the right. Repeating the similar procedure for all exponents, and taking into account

$$\sum_{m=2}^N \sum_{n=1}^{m-1} = \sum_{n=1}^{N-1} \sum_{m=n+1}^N, \quad \text{we obtain}$$

$$\mathcal{T}_k(h, g) = A_k e^{-h\sigma \sum_{n=1}^N \tau'_n} \mathcal{T}_k(0, 0) e^{g\sigma \sum_{n=1}^N \tau''_n} A_k^{-1} \quad (47)$$

$$A_k = \exp \left\{ \sum_{m=2}^N \sum_{n=1}^{m-1} (-h\tau'_m\tau_n - g\tau_m\tau''_n) \right\}$$

Then, due to the charge conservation (46),  $\sum_{n=1}^N \tau_n^{(k)}$  is a constant. For the 6-vertex model this property is known also as the ice rule (see e.g. [1, 9]):

$$\frac{1}{N} \sum_{n=1}^N \tau_n^{(k)} = y_k$$

— the so-called polarization vector.  $y_k$  may take values  $-1 \leq y_k \leq 1$ .

Restoring the index  $k$ ,  $A_k$  can be written as

$$A_k = C_{k+1,k} C_{k,k-1}; \quad C_{k+1,k} = \exp \left\{ \sum_{m=2}^N \sum_{n=1}^{m-1} (-h_k \tau_m^{(k+1)} \tau_n^{(k)}) \right\}$$

Multiplying  $\mathcal{T}_1 \mathcal{T}_2 \dots \mathcal{T}_K$  and using  $A_k^{-1} A_{k+1} = C_{k,k-1}^{-1} C_{k+2,k+1}$ , we get for the global monodromy matrix (9):

$$\mathcal{T} = C_{1,0} C_{2,1} e^{-h_1 \sigma^{(1)} Y_2} \mathcal{T}_1(0, 0) e^{h_0 \sigma^{(1)} Y_0} C_{1,0}^{-1} C_{3,2} \dots C_{K-1,K-2}^{-1} C_{K+1,K} e^{-h_K \sigma^{(K)} Y_{K+1}} \mathcal{T}_K(0, 0) e^{h_{K-1} \sigma^{(K)} Y_{K-1}} C_{K+1,K}^{-1} C_{K,K-1}^{-1}$$

Here  $Y_k = N y_k$ .

Moving  $C$ -factors ( $C^{-1}$ -factors) to the left (to the right), one obtains

$$\mathcal{T} = B \left( \prod_{k=1}^K e^{-h_k \sigma^{(k)} Y_{k+1}} \mathcal{T}_k(0, 0) e^{h_{k-1} \sigma^{(k)} Y_{k-1}} \right) B^{-1} \quad (48)$$

$$B = \prod_{k=1}^K C_{k, k-1}$$

$B$  depends only on  $\tau_n^{(k)}$ , and therefore it is a gauge transformation. In the other hand, one can consider the transfer-matrix for the 6-vertex model in a horizontal field of strength  $H$

$$\mathcal{T}_{6v}(H) = \prod_{n=1}^N e^{-\frac{H}{2}\sigma} L_n e^{-\frac{H}{2}\sigma}$$

Doing the same procedure, we arrive to formula (47) with substitution  $h = -g = H/2$ ;  $\tau'_n, \tau''_n \rightarrow 1$ :

$$\mathcal{T}_{6v}(H) = A e^{-\frac{NH}{2}\sigma} \mathcal{T}_{6v}(0) e^{-\frac{NH}{2}\sigma} A^{-1}$$

in which  $A$  again is a gauge transformation. Comparing the last relation with (48), we see that partition function of our model and the set 6-vertex planes,  $k$ -th plane in a field

$$H_k = h_k y_{k+1} - h_{k-1} y_{k-1}$$

(both systems with open boundaries) are gauge-equivalent. Hence, their transfer-matrices are equal

$$\mathbf{T}_{our\ model} = \prod_{k=1}^K T_{6v}(h_k y_{k+1} - h_{k-1} y_{k-1})$$

## References

- [1] R.J. Baxter, Exactly solvable models in Statistical Mechanics (Academic Press, London, 1982)
- [2] E.H. Lieb, Phys. Rev. **162**, 162 (1967)
- [3] A.B. Zamolodchikov , Soviet JETP **52**, 325 (1980); A.B. Zamolodchikov, Comm. Math, Phys. **79**, 489 (1981)
- [4] V.V. Bazhanov, R.J.Baxter, J.Stat.Phys. **69**, 453 (1992) V. V. Mangazeev, S. M. Sergeev and Yu. G. Stroganov. New series of 3D lattice integrable models., Int. J. Mod. Phys. **A9**, 5517 (1994).
- [5] L.A. Takhtajan and L.D.Faddeev, Uspekhi Mat. Nauk. **34**:5 (1979) 13, translated in Russian Math. Surveys **34**:5 (1979) 11.
- [6] A.E.Borovick, S.I.Kulinich, V.Yu.Popkov, Yu.M.Stzhemechny, Int. J Modern Phys. B, vol. 10, 443-453 (1996).
- [7] V.Yu. Popkov, Anisotropic extension of 2D solvable models of statistics to 3D.// Phys. Lett.A, **192**, 337 (1994).
- [8] V. Popkov, V. Enolskii, M. Salerno, *Exactly solvable multilayered 3D statistical model with competing interactions : connections with ANNNI model*, SNUTP 96-020 - preprint.
- [9] E.H.Lieb, F.Y.Wu: in "*Phase Transitions and Critical Phenomena*",Vol.1 (Exact results). Ed. C.Domb, M.Green; Academic Press, N.Y., 1972, p. 436.
- [10] Pokrovsky V.L. and Talapov A.L. 1980 Sov. Phys. JETP **51**, 134.
- [11] J.D. Noh, D. Kim, Phys.Rev.E **53**,3225 (1996).